Simulation-Based Evaluation of a Positive Pressure Ventilation System for Classroom Air Quality Control under Bangkok Haze Conditions: A CONTAM Simulation Study

Phone Thant Kyaw[1], Roytor Charoensin-O-Larn[2], Saran Salakij[2], Maneerat Ongwandee[4], Kamonchai Yongprapat[5], and Sirima Panyametheekul[1,3*]

[1]Department of Environmental and Sustainable Engineering, Faculty of Engineering, Chulalongkorn University, Bangkok 10330, Thailand
[2]Department of Mechanical Engineering, Faculty of Engineering, Chulalongkorn University, Bangkok 10330, Thailand
[3]Energy Research Institute, Chulalongkorn University, Thailand
[4]Institute of Metropolitan Development, Navamindradhiraj University, Bangkok 10300, Thailand
[5]Academic Service Center for Urbanology, Navamindradhiraj University, Bangkok 10300, Thailand
**Corresponding Author E-mail: sirima.p@chula.ac.th*

ABSTRACT

Educational institutions in rapidly urbanizing tropical cities such as Bangkok increasingly face a critical indoor air quality (IAQ) challenge during seasonal haze episodes—such as the 2025 Bangkok haze event, during which 352 schools were reported closed—when sealing classrooms against fine particulate matter ($PM_{2.5}$) triggers rapid metabolic carbon dioxide (CO_2) accumulation, creating a dual-contaminant crisis under strict tropical energy constraints. This study evaluated positive pressure ventilation system (PPS) configurations for a Bangkok classroom by quantifying the trade-off between indoor air quality and energy use. A CONTAM multizone model was calibrated against measured indoor $PM_{2.5}$ and CO_2 in one monitored Bangkok classroom and independently validated against a second classroom, then applied to a 24-scenario matrix combining Normal and Haze outdoor $PM_{2.5}$ conditions, four airflow rates (3, 4, 5, and 6 ACH), and three filter grades (MERV 11, MERV 13, and HEPA H13). To isolate the effect of outdoor particulate pollution, identical meteorological boundary conditions were applied to both conditions, so that only the outdoor $PM_{2.5}$ profile differed. Performance was assessed by $PM_{2.5}$ reduction, CO_2 control, the percentage of occupied time within the Thai Ministry of Public Health B.E. 2565 guidelines ($PM_{2.5}$ ≤25 μg/m³; CO_2 ≤1,000 ppm), combined IAQ compliance (both guidelines met), the $PM_{2.5}$ indoor-to-outdoor (I/O) ratio, and the total ventilation and cooling energy computed by a time-step enthalpy method from Bangkok weather data; a one-at-a-time sensitivity analysis tested five uncertain model inputs. CO_2 control depended almost entirely on airflow rate: occupied-time compliance rose from about 32% at 3 ACH and 40% at 4 ACH to 96-97% at 5-6 ACH, independent of filter grade. $PM_{2.5}$ control depended on both filter grade and outdoor condition. HEPA kept indoor $PM_{2.5}$ at 9-17 μg/m³ under both conditions (90-100% compliance; I/O 0.10-0.19 under haze), whereas MERV 13 was marginal under the normal condition (20-28 μg/m³; 37-89% compliance) and both MERV grades failed under haze (59-86 μg/m³; ≈1% compliance). Because identical weather was applied to both conditions, the total energy depended only on airflow rate and filter grade (6.5–13.6 kWh per day, dominated by outdoor-air cooling; fan power and filter grade together changed the daily total by less than 5%) and was therefore the same for Normal and Haze operation. HEPA at 5 ACH gave the best overall IAQ-energy balance under both conditions, meeting both guidelines 96% of occupied time at 11.1 kWh per day, whereas 6 ACH added only 1 percentage point for 22% more energy. Indoor $PM_{2.5}$ was most sensitive to the indoor source strength and initial floor loading and least sensitive to envelope leakage and particle penetration, and the HEPA case remained fully compliant in every sensitivity case. These findings support HEPA filtration at about 5 ACH as a single, energy-efficient operating mode, providing practical guidance for climate-resilient classroom ventilation in Bangkok and other Southeast Asian cities affected by seasonal haze.

Keywords: Indoor Air Quality (IAQ) / Energy consumption / $PM_{2.5}$ / CO_2

1. INTRODUCTION

Indoor air quality (IAQ) in educational settings plays a decisive role in students' cognitive function, academic performance, and overall well-being. Children are particularly vulnerable to

airborne hazards because they inhale a greater air volume per unit of body weight than adults and spend roughly 12% of their lives inside school buildings [1]. Poor classroom IAQ is linked to increased absenteeism and the exacerbation of chronic respiratory conditions such as childhood asthma [2], while elevated concentrations of carbon dioxide (CO_2) and fine particulate matter measurably impair concentration, memory, and learning [2, 3].

Bangkok experiences a severe seasonal $PM_{2.5}$ crisis driven by traffic, industry, and agricultural burning, frequently exceeding international safety limits [4]. The urgency was underscored during the January 2025 episode—the 2025 Bangkok Haze Event—when air pollution forced the closure of 352 Bangkok schools across 31 districts on 24 January 2025 [5, 6]. Bangkok classrooms face a two-sided problem: in naturally ventilated rooms indoor air quality is dictated almost entirely by outdoor pollution, exposing students to high $PM_{2.5}$ [4]; in air-conditioned rooms with closed windows, outdoor dust is excluded but inadequate fresh-air supply allows CO_2 to accumulate to 1,700–1,800 ppm, degrading perceived air quality and cognition [4].

A Positive Pressure Ventilation System (PPS) addresses both contaminants at once: by supplying filtered outdoor air it maintains a slight positive indoor pressure that reduces infiltration of unfiltered outdoor $PM_{2.5}$, while the same outdoor-air supply dilutes occupant-generated CO_2. Under Bangkok's hot, humid climate, however, this outdoor-air supply imposes a cooling penalty, so a practical configuration must balance IAQ against energy use [4, 7]. The principal antecedent to this work, Ongwandee et al. (2024), monitored ten indoor spaces in a Bangkok Metropolitan Administration (BMA) secondary school and installed a PPS in a representative classroom [4]. That study reported indoor-to-outdoor $PM_{2.5}$ ratios near unity in naturally ventilated rooms and CO_2 near 2,700 ppm in sealed air-conditioned rooms; after the PPS intervention, indoor $PM_{2.5}$ was held below about 20 μg/m³ during class time and CO_2 fell below roughly 1,200 ppm, but only a single configuration (HEPA at ~3 ACH) under one outdoor condition was evaluated [4, 8, 9].

This study extends that work using multizone simulation. A CONTAM model of the same representative Bangkok classroom was calibrated against the measured PPS dataset and independently validated against a second monitored classroom, then applied to a structured matrix combining two outdoor $PM_{2.5}$ conditions (Normal and Haze), four airflow rates (3, 4, 5, and 6 ACH), and three filter grades (MERV 11, MERV 13, and HEPA H13). Each of the 24 configurations was evaluated for $PM_{2.5}$ reduction, CO_2 control, the percentage of occupied time within the Thai Ministry of Public Health B.E. 2565 guidelines, combined IAQ compliance, and the $PM_{2.5}$ indoor-to-outdoor ratio, together with the total ventilation and cooling energy, and the robustness of the results to uncertain model inputs was tested by a sensitivity analysis. Simulation was preferred over repeated field measurement because the parametric scope would be prohibitive to reproduce and because haze-event outdoor concentrations cannot be recreated experimentally without exposing students to risk [10, 11].

2. METHODOLOGY

2.1 Case-Study Classroom and CONTAM Model

The reference geometry is the BMA classroom monitored by Ongwandee et al. (2024), located in a densely populated residential area of Bangkok about 700 m from the main traffic road [4]. The modeled room ("Classroom 3") has a floor area of 64 m² (8 m × 8 m), a height of 2.9 m, and a net internal air volume of about 173 m³. It is occupied by 20 students and one teacher during class hours, served by two recirculating split-type air conditioners (Daikin, 4.4 kW each; total 8.8 kW; COP ≈ 3.1) and by a PPS that supplies filtered outdoor air through two units; windows and doors are kept closed during operation to maintain positive pressure.

The classroom was represented in CONTAM v3.4 (NIST) as a single well-mixed zone connected to an adjacent corridor and to an outdoor boundary node (Figure 1), with an indoor setpoint of 25 °C and 60% relative humidity [11]. The corridor is a buffer that is open to the outdoors, while the outdoor node carries time-varying weather and pollutant boundary conditions. Airflow through the scheduled

door, closed-door and window-frame leakage, and background envelope leakage was represented with CONTAM's power-law relationship,

$$Q = C(\Delta P)^n$$

Where; Q is the airflow through a leakage path (m^3/s), C the flow coefficient, ΔP the pressure difference (Pa), and n the pressure exponent. Effective leakage areas were assigned from blower-door measurements in 12 school classrooms (corridor-side ELA ≈ 264.7 cm^2 for the classroom–corridor partition; outdoor-side ELA ≈ 93.1 cm^2 for the exterior window and wall) [23], and the corridor–outdoor connection as a two-way single opening, following the ASHRAE Handbook—Fundamentals and CONTAM documentation [11, 12]. Outdoor meteorological inputs were taken from the Bangkok EPW weather file [13], while outdoor $PM_{2.5}$ was supplied separately from measured air-quality data.

The PPS supply airflow follows:

$$Q = \frac{ACH \times V}{3600}$$

Where; V is the classroom volume; the four target rates of 3, 4, 5, and 6 ACH correspond to PPS supply flows of 540, 720, 900, and 1,080 m^3/h (two units), i.e., actual air-change rates of about 3.1-6.2 h^{-1}. Three filter grades were modeled—MERV 11 (ISO ePM_{10} 70%), MERV 13 (ISO ePM_1 55%), and HEPA H13 (≥99.95% at MPPS)—with removal efficiencies applied at the PPS supply path following ANSI/ASHRAE Standard 52.2 and EN 1822, and with airflow-dependent pressure drops used for the fan-energy calculation [9, 16]. Key model inputs are summarized in Table 3.

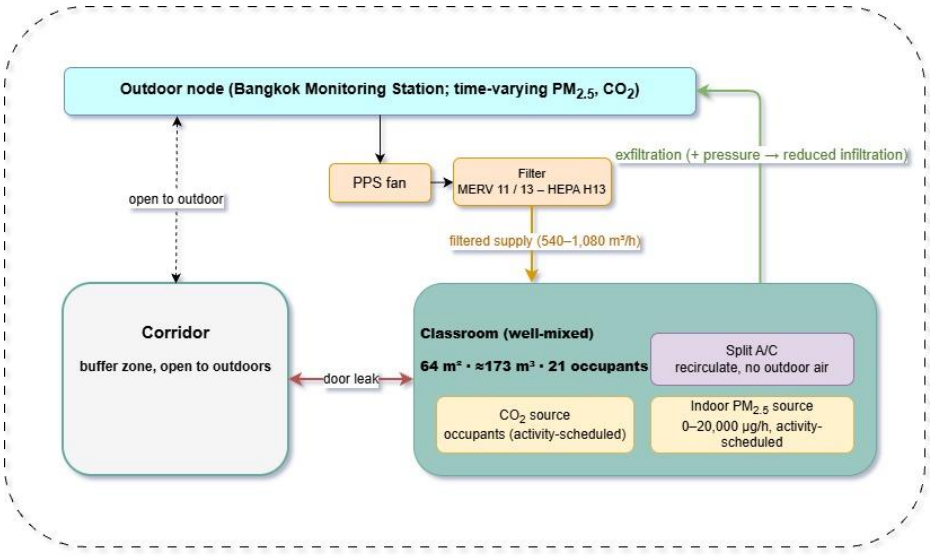

Figure 1. Schematic of the three-zone CONTAM model (outdoor node, corridor, and well-mixed classroom) showing the PPS supply through the filter, occupant and indoor sources, and pressure-driven airflow paths.

2.2 Indoor Contaminant Sources

Two contaminants were modeled. CO_2 was represented as an occupant-generated source applied on the time-varying occupancy schedule of Table 1. The occupant CO_2 generation rate was assumed to be 0.006 L/s per person. Persily and de Jonge (2017) reported a CO_2 generation rate of 0.0056 L/s per person for light sitting activity at 1.5 met [14], while adolescent-specific calculations based on Wu et al. (2023) give approximately 0.0066 L/s for a 15-year-old occupant at the same activity level [15].

Therefore, 0.006 L/s per person was adopted as a representative value for classroom occupants under light activity conditions. A constant outdoor CO_2 concentration of 420 ppm was assumed.

Indoor $PM_{2.5}$ generation was represented as an activity-dependent classroom source to account for particle generation and resuspension associated with student occupancy, movement, chalk use, and cleaning activities. A baseline source strength of 5,000 µg/h was assigned during normal seated occupancy, consistent with the classroom source adopted by Won et al. (2026) and comparable to the mean net indoor $PM_{2.5}$ source of approximately 4.8 mg/h reported for chalkboard-equipped public-school classrooms by Alameddine et al. (2022) [9, 22]. To represent increased resuspension with occupant activity, source strengths of 7,500 and 10,000 µg/h were assigned to light- and heavy-movement periods, the latter corresponding to the 200% high-activity condition of Won et al. (2026). A short end-of-day peak of 20,000 µg/h was applied during classroom cleaning, when students erased and dusted the chalkboard and disturbed settled dust; this transient high-resuspension condition is of the same order as the upper net-source range (up to ≈15.9 mg/h) reported by Alameddine et al. (2022) and is consistent with field observations in which indoor $PM_{2.5}$ rose to approximately 35 µg/m³ near the end of the school day. Because CONTAM schedule multipliers are bounded between 0 and 1, the maximum source strength was defined as 20,000 µg/h and the activity schedule (Table 2) was normalized relative to this value. Indoor $PM_{2.5}$ losses were represented by deposition onto the 64 m² floor at a deposition velocity of 1.5×10^{-4} m/s (equivalent to 0.2 h^{-1}, consistent with the 0.19 h^{-1} adopted for $PM_{2.5}$ in building simulations and the 0.22-0.32 h^{-1} measured for 0.3-3 µm particles in classrooms [23, 24]), with first-order resuspension of the deposited mass (0.01 h^{-1}, of the order of the 10^{-2}-10^{-3} h^{-1} reported for walking-induced $PM_{2.5}$ resuspension [25]) from an initial floor loading L(0) of 30 mg/m², treated as a calibration parameter and tested in the sensitivity analysis (Section 2.6), while outdoor $PM_{2.5}$ entered through envelope leakage, with a penetration factor P = 0.8 [21, 23, 24, 26], and through the PPS supply after filtration.

Table 1. Classroom occupancy and activity schedule for Classroom 3 (calibration and scenarios) and Classroom 1 (validation); the analysis period is 09:30-15:30 (Section 2.4)

Time	Activity	Classroom 3 (calibration and scenarios)		Classroom 1 (validation)	
		Occupants	Doors	Occupants	Doors
08:30-09:20	Class	21 (20 + teacher)	Closed	23 (22 + teacher)	Closed
09:20-09:30	Break	20	Open/Close	22	Open/Close
09:30-10:10	Class	21 (20 + teacher)	Closed	23 (22 + teacher)	Closed
10:10-11:00	No Class (Classroom 3); Class (Classroom 1)	0	Closed	23 (22 + teacher)	Closed
11:00-11:50	Lunch break	0	Open/Close	0	Open/Close
11:50-12:40	Class	21 (20 + teacher)	Closed	23 (22 + teacher)	Closed
12:40-12:50	Break	20	Open/Close	22	Open/Close
12:50-13:25	Class	21 (20 + teacher)	Closed	23 (22 + teacher)	Closed
13:25-13: 35	Break	20	Open/Close	22	Open/Close
13:35-14:15	Class	21 (20 + teacher)	Closed	23 (22 + teacher)	Closed
14:15-14:25	Break	20	Open/Close	22	Open/Close
14:25-15:10	Class	21 (20 + teacher)	Closed	23 (22 + teacher)	Closed
15:10-15:30	Class end / cleaning	20	Open/Close	22	Open/Close

Table 2. Indoor $PM_{2.5}$ source strength by classroom activity (normalized to the 20,000 µg/h maximum)

Classroom activity	$PM_{2.5}$ source (µg/h)	Schedule multiplier
Unoccupied	0	0.00
Normal seated class	5,000	0.25
Light movement	7,500	0.375

Table 2. Indoor $PM_{2.5}$ source strength by classroom activity (normalized to the 20,000 µg/h maximum) (cont.)

Classroom activity	$PM_{2.5}$ source (µg/h)	Schedule multiplier
Heavy movement / return from lunch	10,000	0.50
Cleaning / chalkboard erasing and dusting	20,000	1.00

Table 3. Key model inputs and pollutants, deposition, and filter assumptions

Parameter	Value / assumption	Basis
Room air volume	64 m² floor × 2.9 m; ≈173 m³	Site
Indoor setpoint	25 °C, 60% RH	Model
Occupants	20 students + 1 teacher (Classroom 3); 22 + 1 (Classroom 1)	Ongwandee [4]
Occupant CO_2 generation	~0.006 L/s per occupant	Persily [14]; Wu[15]
Outdoor CO_2	420 ppm (constant)	Model
Indoor $PM_{2.5}$ source	0–20,000 µg/h (activity-scheduled)	Won [9] ; Alameddine [22]
Deposition	1.5×10^{-4} m/s (≈0.2 h^{-1})	Won [9]; model
Resuspension	0.01 h^{-1} (first order)	Benabed [25]; calibrated
Initial floor loading, L(0)	30 mg/m²	Calibrated
Effective leakage area	264.7 cm² (corridor side); 93.1 cm² (outdoor side)	Eom [23]
Particle penetration (leakage)	P = 0.8	Eom [23]; Chen & Zhao [21]
Filter grades	MERV 11 (ePM_{10} 70%), MERV 13 (ePM_1 55%), HEPA H13 (≥99.95%)	ASHRAE 52.2 [16]
PPS supply airflow	540 / 720 / 900 / 1,080 m³/h (3–6 ACH)	Design
Fan efficiency	0.50 (total static)	Assumed
A/C units	2 × 4.4 kW split; COP ≈ 3.1	Product data
Initial Indoor State (09:30)	CO_2 ≈ 1,151 ppm; $PM_{2.5}$ ≈ 21 µg/m³	Measured
Simulation period	09:30–15:30 (6 h; monitored period), 5-min step	Monitoring

2.3 Model Calibration and Validation

The model was calibrated and validated in two steps against the monitored PPS condition (HEPA filtration at ~3 ACH) [4]. First, it was calibrated against the indoor CO_2 and $PM_{2.5}$ measured in Classroom 3 on 11 November 2022 at 5-minute resolution: the uncertain indoor-particle inputs—the resuspension rate, the initial floor loading L(0), and the indoor $PM_{2.5}$ source schedule—were adjusted within physically plausible ranges, whereas envelope leakage, particle penetration, and deposition were taken from field measurements and the literature (Table 3) and were not adjusted, and the calibrated parameter set was then fixed. Second, without further adjustment, the fixed parameter set was applied to Classroom 1, monitored on 10 November 2022, changing only the room- and day-specific inputs (occupancy, activity and door schedule, outdoor boundary concentrations, and initial indoor concentrations); this comparison provides an independent validation. The simulation and compliance evaluation covered 09:30–15:30, the period for which measured indoor CO_2 and $PM_{2.5}$ data were available on the monitored day [4]; the first class period (08:30–09:30) was therefore excluded from the reported metrics. Agreement was quantified from the paired five-minute values (n = 72 and 70 on the calibration and validation days) by the root-mean-square error, $RMSE = [\Sigma(S_i - M_i)^2/n]^{1/2}$, the normalized mean bias error, $NMBE = \Sigma(S_i - M_i)/[(n-1)\cdot M_{mean}] \times 100$, the coefficient of variation of the RMSE, $CV(RMSE) = [\Sigma(S_i - M_i)^2/(n-1)]^{1/2}/M_{mean} \times 100$, and the relative mean absolute error, $RMAE = \Sigma|S_i - M_i|/(n\cdot M_{mean}) \times 100$, where S_i and M_i are the simulated and measured values and M_{mean} is the measured mean, and was judged against the ASHRAE Guideline 14 criteria for calibrated simulation ($|NMBE| \leq 10\%$; $CV(RMSE) \leq 30\%$) [17, 18]. As summarized in Table 4 and Figure 2, CO_2 was reproduced closely on both days (NMBE −1.3% and −4.8%; CV(RMSE) 4.2% and 6.7%; $R^2 = 0.98$ and 0.94 for the calibration and validation days, respectively), and $PM_{2.5}$ also met both criteria (NMBE −5.3% and −3.2%; CV(RMSE) 21.3% and 26.4%; RMAE 16.8% and 18.8%). Its temporal correlation

was weaker (R^2 = 0.46 and 0.35) because short activity-driven peaks are captured less precisely than the mean level. The occupied-period means, which are the basis of the compliance percentages, are therefore treated as the primary results, while statements about short transient peaks, such as the end-of-day cleaning spike, should be read as qualitative.

Because each comparison covers a single school day in a classroom operated with HEPA filtration at about 3 ACH under moderate outdoor $PM_{2.5}$, the scenario predictions for MERV filters, higher airflow rates, and haze-level outdoor concentrations are extrapolations beyond the measured conditions. These predictions rest on the same mass-balance structure, with filter efficiencies taken from standard test data rather than fitted, so the relative ranking of configurations is expected to be more reliable than the absolute concentrations, given the moderate $PM_{2.5}$ correlation, the occupied-period means and compliance percentages are treated as the primary results, while predicted short-term peaks (e.g., during end-of-day cleaning) are interpreted qualitatively; the agreement on an independent day and room nonetheless supports the use of the model for the parametric analysis that follows. The effect of the remaining input uncertainty on the predictions was examined by the sensitivity analysis in Section 2.6.

Table 4. Calibration (Classroom 3, 11 Nov 2022) and independent validation (Classroom 1, 10 Nov 2022): measured versus simulated five-minute values, 09:30–15:30 (n = 72 and 70)

Metric	Calibration-Classroom 3		Validation-Classroom 1		ASHRAE G14
	CO_2 (ppm)	$PM_{2.5}$ (µg/m³)	CO_2 (ppm)	$PM_{2.5}$ (µg/m³)	criterion
Measured mean	1,041	17.5	1,256	18.5	–
Simulated mean	1,028	16.6	1,197	17.9	–
RMSE	43.3	3.71	83.5	4.83	–
NMBE (%)	-1.3	-5.3	-4.8	-3.2	±10
CV (RMSE) (%)	4.2	21.3	6.7	26.4	≤30
RMAE (%)	3.2	16.8	5.8	18.8	–
R^2	0.98	0.46	0.94	0.35	–

2.4 Simulation Scenario Matrix

The calibrated and validated model was applied to a full-factorial matrix of two outdoor $PM_{2.5}$ conditions, four airflow rates, and three filter grades, giving 24 scenarios (Table 5). The Normal condition used measured Bangkok outdoor $PM_{2.5}$ data for 23 June 2022 (occupied-hour mean ≈ 21 µg/m³), and the Haze condition used 24 January 2025 (occupied-hour mean ≈ 92 µg/m³, with class-hour peaks near 134 µg/m³ and an early-morning peak of about 146 µg/m³). To isolate the influence of elevated outdoor $PM_{2.5}$, identical meteorological boundary conditions—outdoor temperature, relative humidity, wind speed, and wind direction—were applied to both conditions, and only the outdoor $PM_{2.5}$ profile was varied (Figure 3). This controlled design ensures that differences in indoor air quality and in ventilation-related cooling energy are attributable to the ventilation and filtration strategies and to the outdoor $PM_{2.5}$ level, rather than to differences in weather between separate historical days. Geometry, leakage, air-conditioning, and the occupancy schedule were held constant so that differences arose only from the three controlled factors; all cases used fixed-airflow PPS operation, starting from the indoor state measured in Classroom 3 at 09:30 (CO_2 ≈ 1,151 ppm; $PM_{2.5}$ ≈ 21 µg/m³), which carries over from the first class period.

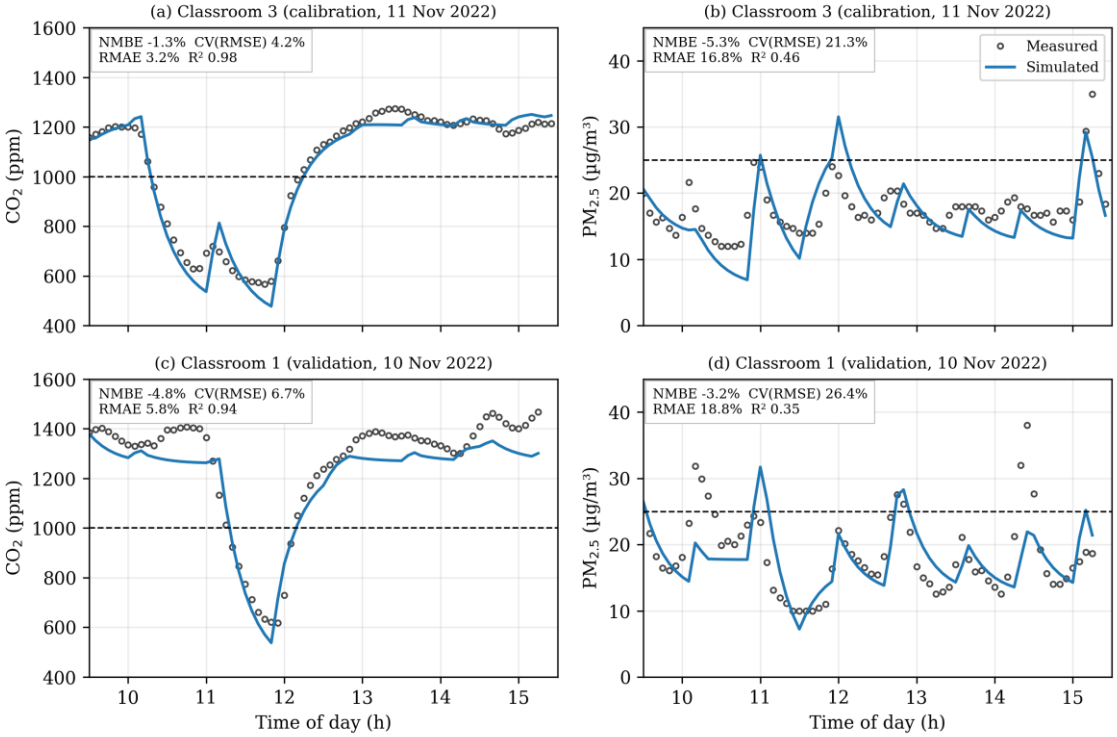

Figure 2. Measured versus simulated five-minute CO_2 (a, c) and $PM_{2.5}$ (b, d) time series for the calibration day (Classroom 3; a, b) and the independent validation day (Classroom 1; c, d), with the ASHRAE Guideline 14 metrics for each series. Dashed lines mark the Thai MOPH guidelines.

The representative Normal-condition profile was selected from the 2022 Thonburi District hourly monitoring dataset. Hourly $PM_{2.5}$ data were aggregated into daily averages, and only weekdays with 24 valid hourly records and a daily mean $PM_{2.5} \leq 37.5$ µg/m³ were retained as normal-condition candidates. The median daily $PM_{2.5}$ of these eligible days was computed, and the day whose daily mean was closest to this median was selected, avoiding an unusually clean or extreme day and providing a representative outdoor condition for the simulation.

Table 5. Simulation scenario matrix (2 × 4 × 3 = 24 scenarios)

Factor	Levels
Outdoor $PM_{2.5}$ condition	Normal (23 Jun 2022); Haze (24 Jan 2025)
Airflow rate (fixed)	3, 4, 5, and 6 ACH (540-1,080 m³/h)
Filter grade	MERV 11; MERV 13; HEPA H13
Meteorology	Identical for both conditions (only outdoor $PM_{2.5}$ differs)
Held constant	Geometry, envelope leakage, split A/C, occupancy schedule

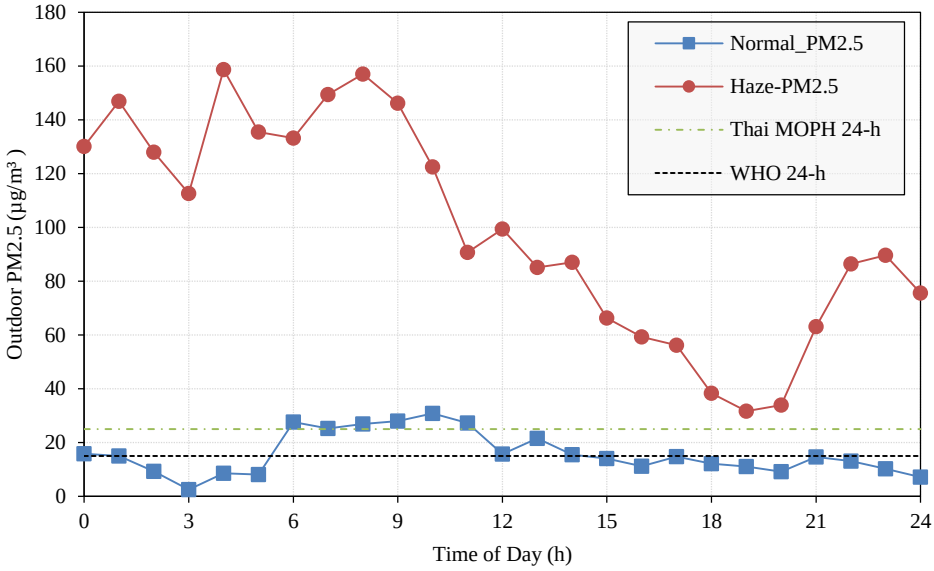

Figure 3. Outdoor $PM_{2.5}$ boundary profiles for the Normal (23 Jun 2022) and Haze (24 Jan 2025) conditions over the simulated day; the shaded band marks the occupied period and the dash-dot and dashed lines mark the Thai MOPH (25 µg/m³) and WHO (15 µg/m³) 24-hour $PM_{2.5}$ guidelines, respectively. Meteorological conditions were identical for both conditions; only the outdoor $PM_{2.5}$ profile differs.

2.5 Energy and Performance Metrics

The total ventilation and cooling energy of each scenario was computed from the PPS supply airflow and the Bangkok hourly weather. The PPS fan energy is:

$$E_{fan} = \frac{Q \times \Delta P \times t}{1000 \times \eta_{fan}}$$

With fan efficiency η_{fan} = 0.50 and filter-specific pressure drop ΔP. Because Bangkok outdoor air carries a large latent load, the cooling of the incoming outdoor air was evaluated on an enthalpy basis at each time step and summed over the coefficient of performance (COP ≈ 3.1) [12]:

$$E_{cooling} = \sum_{t=1}^{n} \frac{\dot{m} \times (h_{out,t} - h_{in,set}) \times \Delta t}{COP}$$

With the load set to zero whenever the outdoor enthalpy is at or below the indoor setpoint enthalpy, and the total energy $E_{total} = E_{fan} + E_{cool}$. Because identical meteorological conditions were applied to both pollution conditions, this energy demand is a function of airflow rate and filter grade only, allowing the ventilation-related energy of the scenarios to be compared under equivalent thermal boundary conditions. IAQ performance was quantified by the compliance metric reported for every scenario—the percentage of occupied five-minute time steps within the applicable guideline value,

$$\text{Compliance (\%)} = \frac{N_{within}}{N_{total}} \times 100 = (1 - \frac{t_{exceed}}{t_{occupied}}) \times 100$$

Where; N_{within} is the number of occupied five-minute time steps with concentration at or below the guideline, N_{total} (= 73) is the total number of occupied time steps over the 09:30-15:30 period, and t_{exceed} is the accumulated exceedance time; this is the definition used for the CO_2 and $PM_{2.5}$ compliance values reported for every scenario. The metric was evaluated against the Thai Ministry of Public Health

B.E. 2565 guidelines ($PM_{2.5} \leq 25$ µg/m³, 24-hour; $CO_2 \leq 1{,}000$ ppm), with the WHO 24-hour $PM_{2.5}$ value of 15 µg/m³ as an additional reference [19, 20]. Because the $PM_{2.5}$ guideline is defined as a 24-hour average, the 5-minute metric is not a formal regulatory compliance assessment; it is used as an exposure-time indicator of how often occupants were exposed above the guideline value during school hours, and is conservative relative to a 24-hour average. The occupied-period mean concentration, which is closer to the averaging basis of the guideline, is therefore reported alongside it (Table 6). The effectiveness of the filtered positive-pressure system in excluding outdoor particles was expressed by the indoor-to-outdoor ratio $I/O = C_{in} / C_{out}$, computed over the occupied period, where a lower value indicates stronger protection [21]. Because indoor $PM_{2.5}$ in this study includes both outdoor-origin particles and the activity-dependent indoor source, this is an apparent (total) I/O ratio that reflects the penetration and filtration of outdoor particles together with indoor generation; values above unity therefore indicate that the indoor source exceeds the outdoor contribution, not net ingress of outdoor particles [21]. To separate the two contributions, the occupied-period mean indoor concentration was expressed as the sum of an outdoor-origin and a non-outdoor component [21, 27, 28]:

$$C_{in} = F_{inf} \times C_{out} + C_{gen}$$

Where; F_{inf} is the outdoor-origin I/O ratio (infiltration factor), i.e. the fraction of outdoor $PM_{2.5}$ that reaches the classroom through the filtered PPS supply and the unfiltered leakage and door paths, and C_{gen} is the non-outdoor component (indoor generation, resuspension, and the common initial condition). Because CONTAM contaminant transport is linear [11] and the Normal and Haze cases of each configuration differ only in the outdoor $PM_{2.5}$ profile, C_{gen} cancels between the two conditions, giving.

$$F_{inf} = \frac{C_{in,Haze} - C_{in,Normal}}{C_{out,Haze} - C_{out,Normal}}$$

With C_{gen} then obtained from Equation (6) for the Normal case, using occupied-period outdoor means of 21 and 92 µg/m³. F_{inf} and C_{gen} are therefore single values for each filter–airflow configuration (Table 6).

Two further indicators were derived for each scenario. The reduction relative to the field-tested baseline (HEPA, 3 ACH) under the same outdoor condition was $R\ (\%) = (1 - C_s/C_{base}) \times 100$, applied to the occupied-period mean $PM_{2.5}$ and CO_2, where negative values denote an increase. Combined IAQ compliance was the percentage of occupied five-minute time steps in which $CO_2 \leq 1{,}000$ ppm and $PM_{2.5} \leq 25$ µg/m³ were met simultaneously. The overall best configuration was defined as the configuration with the lowest daily total energy among those achieving at least 95% combined IAQ compliance.

2.6 Sensitivity Analysis

A one-at-a-time (OAT) sensitivity analysis was performed on two representative cases: Normal-MERV 13-5 ACH, a marginal configuration, and Haze-HEPA-6 ACH, a protective configuration. Five uncertain inputs were varied individually between Low and High levels while all others were held at their base values: the indoor $PM_{2.5}$ source strength (±25%; 15,000 and 25,000 µg/h maximum), the envelope leakage area (×0.75 and ×1.25), the particle penetration factor of the leakage paths (P=0.6 and 1.0; base 0.8), the deposition rate (0.1 and 0.3 h^{-1}; base 0.2 h^{-1}), and the initial floor $PM_{2.5}$ loading L(0) (20 and 40 mg/m²; base 30 mg/m²). Each case required one base and ten Low/High simulations (22 in total), and the response was expressed as the change in occupied-period mean $PM_{2.5}$ and $PM_{2.5}$ compliance relative to the base.

3. RESULTS AND DISCUSSION

3.1 CO_2 Control and Ventilation Adequacy

Because the two split air conditioners only recirculate room air, CO_2 control was governed entirely by the PPS outdoor-air supply and was therefore essentially identical across filter grades and outdoor conditions (Figure 4). At the field-tested rate of 3 ACH the occupied-period mean CO_2 was 1,044 ppm with a peak of 1,283 ppm, and only 32% of occupied time lay below the 1,000-ppm guideline—confirming that ~3 ACH is a minimum rather than a sufficient rate. Raising the airflow lifted compliance only modestly at 4 ACH (40%; mean 900 ppm), because the class-period plateau remained just above 1,000 ppm, but sharply at 5 and 6 ACH (96% and 97%), as the mean CO_2 fell to 810 and 749 ppm—a reduction of 22–28% relative to the 3-ACH baseline. A rate of at least 5 ACH was thus required for reliable CO_2 control [4, 9].

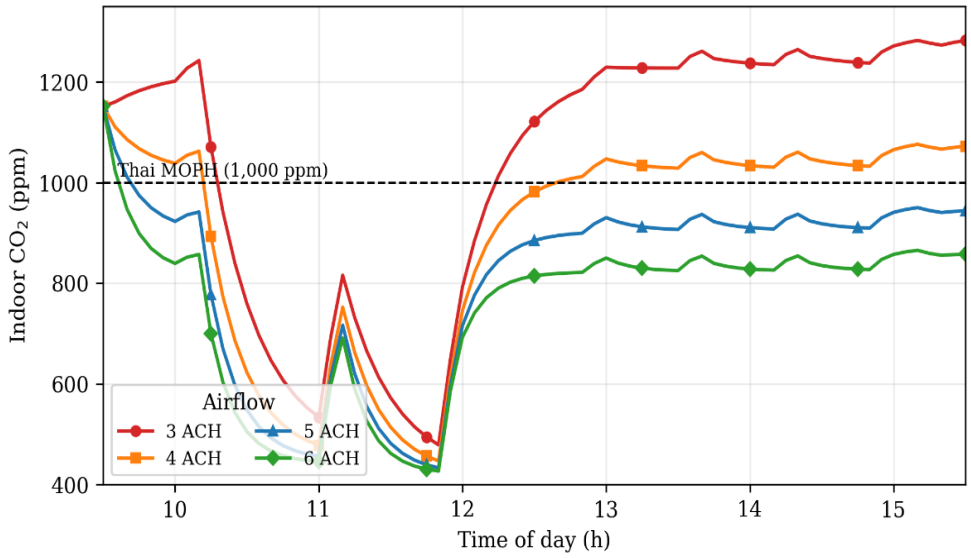

Figure 4. Simulated indoor CO_2 time series over the occupied period at each airflow rate (identical across filter grades and outdoor conditions). The dashed line is the 1,000-ppm guideline; concentrations dip during the mid-morning break and lunch and rebuild during class.

3.2 $PM_{2.5}$ Control and Indoor-to-Outdoor Ratio

In contrast to CO_2, $PM_{2.5}$ control depended strongly on both filter grade and outdoor condition (Figures 5-7).

Under the Normal condition (occupied-hour outdoor mean ≈ 21 µg/m³, Figure 5), HEPA held indoor $PM_{2.5}$ between 9.1 and 16.9 µg/m³ with 92-100% compliance and an I/O ratio falling from 0.82 to 0.44 as airflow increased, a 22-46% reduction relative to the 3-ACH baseline; MERV 13 kept indoor $PM_{2.5}$ at 20.3-27.5 µg/m³ (37-89% compliance, never fully compliant), while MERV 11 exceeded the guideline on average (25.3-32.3 µg/m³; only 4-48% compliance) because its lower fine-particle efficiency admitted more outdoor particles. The I/O ratios above unity for MERV 11 (1.22-1.56) and for MERV 13 at 3-5 ACH (1.05-1.33) reflect the indoor source added to the low Normal-day outdoor concentration rather than a failure of the positive-pressure barrier. Separating the two contributions (Equations 6-7) confirms this: the outdoor-origin I/O ratio (F_{inf}) was well below unity for all filters—0.004-0.006 for HEPA, 0.52-0.55 for MERV 13, and 0.75-0.79 for MERV 11—whereas the non-outdoor component was nearly identical across filters, decreasing from about 17 µg/m³ at 3 ACH to 9 µg/m³ at 6 ACH as the supply air diluted the indoor source (Table 6).

Under the Haze condition (occupied-hour outdoor mean ≈ 92 µg/m³, Figure 6) the differences widened dramatically. MERV 11 and MERV 13 were overwhelmed, with mean indoor $PM_{2.5}$ of about 82-86 and 59-64 µg/m³ respectively and compliance near zero, whereas HEPA suppressed the outdoor contribution to a mean of 9.4-17.3 µg/m³ and an I/O ratio of just 0.10-0.19—four to nine times lower than those of the lower grades. With HEPA, compliance was 90% at 3 ACH and reached 100% at 5-6 ACH, and indoor concentrations were nearly identical to those under the Normal condition (Figure 7), showing that the indoor source rather than outdoor infiltration (F_{inf} ≈ 0.005, i.e. about 0.5 µg/m³ of outdoor origin) controlled the residual $PM_{2.5}$; increasing the airflow diluted this source and reduced the mean by 22-46% relative to the 3-ACH baseline. Thus, during haze episodes HEPA filtration is necessary, and its benefit increases with airflow [4, 9, 21].

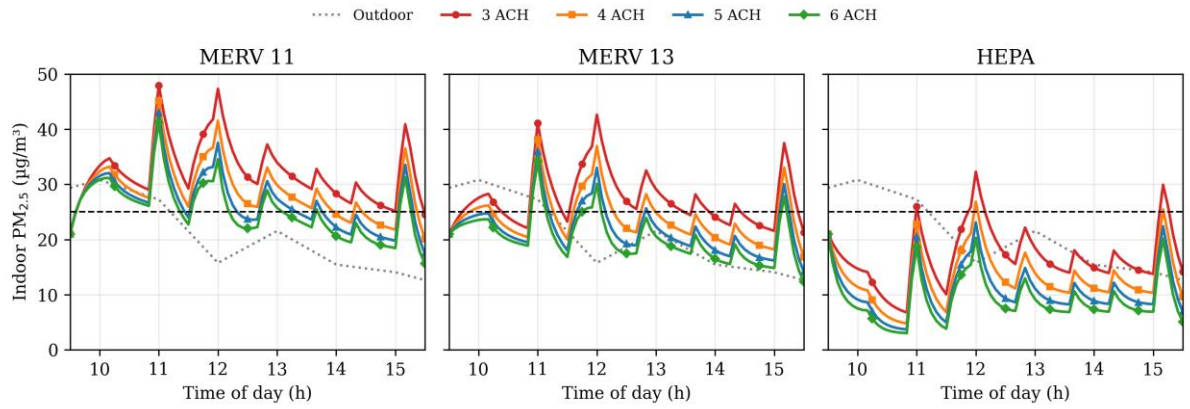

Figure 5. Simulated indoor $PM_{2.5}$ time series under the Normal condition for each filter grade and airflow rate; the dotted line is the outdoor profile and the dashed line the 25 µg/m³ guideline. Peaks reflect door opening around lunch and activity- and cleaning-related resuspension.

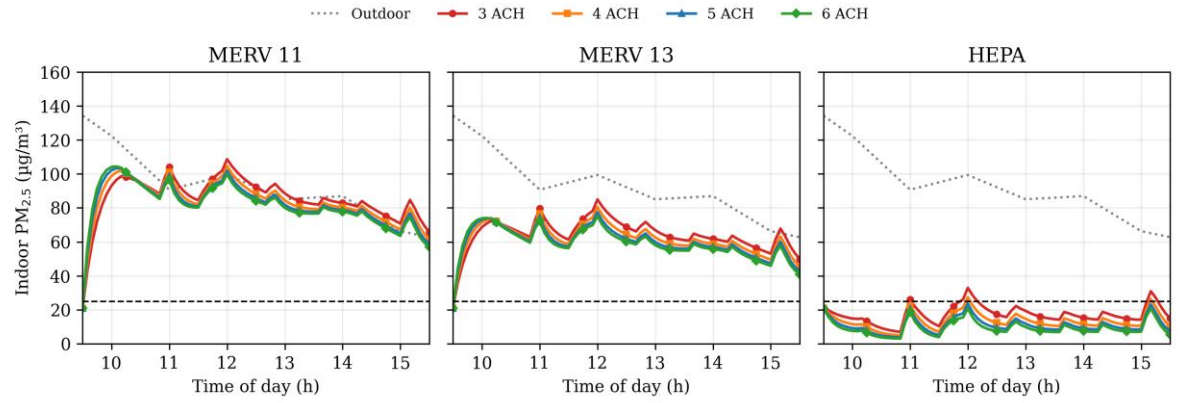

Figure 6. Simulated indoor $PM_{2.5}$ time series under the Haze condition for each filter grade and airflow rate (as Figure 5); only HEPA keeps indoor $PM_{2.5}$ near or below the 25 µg/m³ guideline.

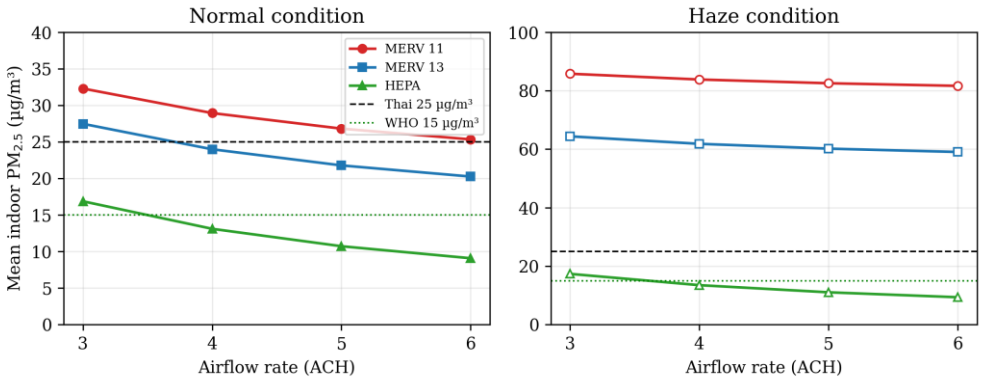

Figure 7. Summary of mean indoor $PM_{2.5}$ versus airflow rate for all three filter grades under the (left) Normal and (right) Haze conditions.

3.3 Energy Trade-offs

The total ventilation and cooling energy were dominated by the cooling of outdoor air, not by fan power (Figure 8a). Fan energy remained below about 0.63 kWh per day even for HEPA at 6 ACH, so the choice of filter grade changed the daily total by less than 5%; the added pressure drop of HEPA is therefore a minor energy penalty at classroom scale. Cooling energy rose with airflow because more outdoor air must be conditioned, increasing the daily total from 6.5 kWh at 3 ACH to 13.6 kWh at 6 ACH. Because identical meteorological conditions were applied to both pollution conditions, this energy demand was the same for Normal and Haze operation: the total ventilation and cooling energy is governed by the airflow rate—and, marginally, the filter grade—not by the outdoor $PM_{2.5}$ level. This isolation is deliberate; it ensures that energy differences between scenarios reflect the ventilation and filtration strategy rather than differences in outdoor temperature and humidity between separate historical days.

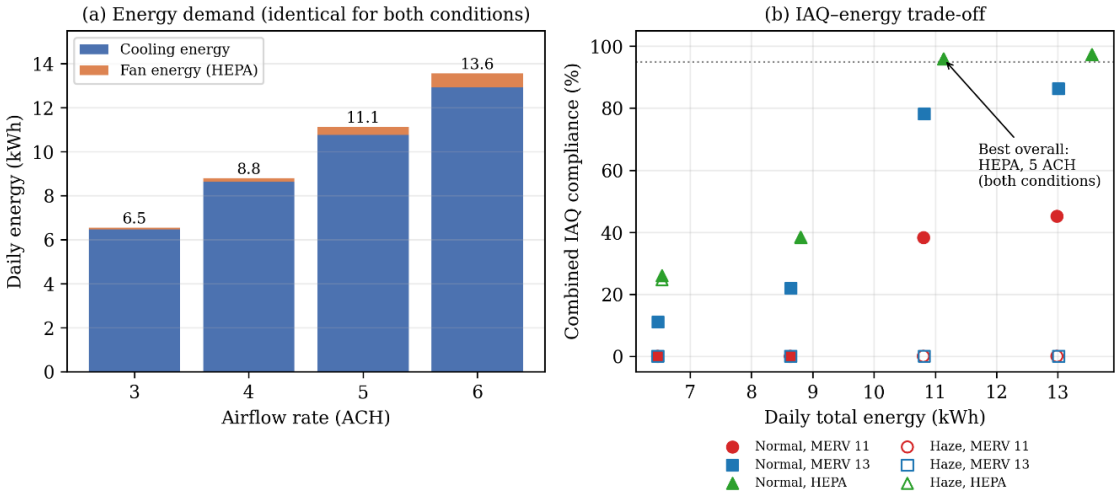

Figure 8. (a) Daily total ventilation and cooling energy versus airflow rate (identical for both conditions; fan component shown for HEPA), and (b) the IAQ–energy trade-off, showing combined IAQ compliance (CO_2 and $PM_{2.5}$ both met) versus daily total energy for all 24 scenarios; the dotted line marks 95%.

The consequence is a clear IAQ-energy trade-off (Figure 8b). Higher airflow improves both CO_2 and $PM_{2.5}$ compliance but raises cooling energy roughly linearly, whereas filter grade shifts $PM_{2.5}$ compliance substantially at almost no energy cost. In terms of combined IAQ compliance, HEPA rose from 25-26% at 3 ACH and 38% at 4 ACH to 96% at 5 ACH and 97% at 6 ACH under both conditions, whereas MERV 13 reached at most 86% (Normal, 6 ACH), MERV 11 at most 45%, and neither MERV grade met both guidelines under haze (Table 6). HEPA at 5 ACH was therefore the best overall

configuration under both conditions (96% combined compliance at 11.1 kWh per day); moving to 6 ACH added only 1 percentage point for 2.4 kWh (22%) more energy.

Table 6. Summary of simulated IAQ and energy results for all 24 scenarios (fixed-airflow PPS; occupied period). Reduction relative to the HEPA-3 ACH baseline of the same condition (negative = increase); Both = CO_2 and $PM_{2.5}$ guidelines met simultaneously; bold = best overall. F_{inf} = outdoor-origin I/O ratio; C_{gen} = non-outdoor component (μg/m³) (Equations 6-7)

Cond.	Filter	ACH	CO_2 mean (ppm)	CO_2 ≤1000 (%)	CO_2 red. (%)	$PM_{2.5}$ mean (μg/m³)	$PM_{2.5}$ ≤25 (%)	$PM_{2.5}$ red. (%)	I/O	F_{inf}	C_{gen} (μg/m³)	Both met (%)	Energy (kWh)
Normal	HEPA	3	1,044	32	0	16.9	92	0	0.82	0.006	16.8	26	6.54
Normal	HEPA	4	900	40	+14	13.1	97	+22	0.63	0.006	13.0	38	8.80
Normal	**HEPA**	**5**	**810**	**96**	**+22**	**10.7**	**100**	**+36**	**0.52**	**0.004**	**10.6**	**96**	**11.14**
Normal	HEPA	6	749	97	+28	9.1	100	+46	0.44	0.004	9.0	97	13.56
Normal	MERV 13	3	1,044	32	0	27.5	37	−63	1.33	0.520	16.6	11	6.47
Normal	MERV 13	4	900	40	+14	24.0	68	−42	1.16	0.532	12.8	22	8.64
Normal	MERV 13	5	810	96	+22	21.8	82	−29	1.05	0.541	10.4	78	10.82
Normal	MERV 13	6	749	97	+28	20.3	89	−20	0.98	0.546	8.8	86	13.01
Normal	MERV 11	3	1,044	32	0	32.3	4	−91	1.56	0.754	16.5	0	6.47
Normal	MERV 11	4	900	40	+14	28.9	21	−72	1.40	0.773	12.7	0	8.64
Normal	MERV 11	5	810	96	+22	26.8	41	−59	1.30	0.786	10.3	38	10.81
Normal	MERV 11	6	749	97	+28	25.3	48	−50	1.22	0.794	8.6	45	12.98
Haze	HEPA	3	1,044	32	0	17.3	90	0	0.19	0.006	16.8	25	6.54
Haze	HEPA	4	900	40	+14	13.5	97	+22	0.15	0.006	13.0	38	8.80
Haze	**HEPA**	**5**	**810**	**96**	**+22**	**11.0**	**100**	**+36**	**0.12**	**0.004**	**10.6**	**96**	**11.14**
Haze	HEPA	6	749	97	+28	9.4	100	+46	0.10	0.004	9.0	97	13.56
Haze	MERV 13	3	1,044	32	0	64.4	1	−271	0.70	0.520	16.6	0	6.47
Haze	MERV 13	4	900	40	+14	61.8	1	−256	0.67	0.532	12.8	0	8.64
Haze	MERV 13	5	810	96	+22	60.2	1	−247	0.65	0.541	10.4	0	10.82
Haze	MERV 13	6	749	97	+28	59.1	1	−240	0.64	0.546	8.8	0	13.01
Haze	MERV 11	3	1,044	32	0	85.8	1	−395	0.93	0.754	16.5	0	6.47
Haze	MERV 11	4	900	40	+14	83.8	1	−383	0.91	0.773	12.7	0	8.64
Haze	MERV 11	5	810	96	+22	82.6	1	−376	0.90	0.786	10.3	0	10.81
Haze	MERV 11	6	749	97	+28	81.7	1	−371	0.89	0.794	8.6	0	12.98

3.4 Design Implications

Taken together, the results define a clear operating strategy. HEPA at about 5 ACH offered the best balance under both conditions—meeting the CO_2 and $PM_{2.5}$ guidelines simultaneously 96% of the time at roughly 11.1 kWh per day—so a single operating mode can serve both normal and haze days without changing filters. MERV 13 at 5–6 ACH was adequate for CO_2 but met the $PM_{2.5}$ guideline only 82–89% of the time under normal conditions, MERV 11 was inadequate for particles, and neither MERV grade provided meaningful protection during haze. The remaining non-compliant time at 5 ACH occurred at the start of the period, when CO_2 carried over from the first class period still exceeded 1,000 ppm, while at lower airflow the simulated $PM_{2.5}$ exceedances occurred mainly around door-opening and end-of-day cleaning periods (a qualitative indication, given the model's weaker tracking of short peaks), indicating that operational measures—minimizing door openings and managing indoor particle generation, particularly during end-of-day cleaning—are needed alongside filtration. Because identical weather was applied to both conditions, HEPA operation during haze carries the same cooling-energy demand as normal-day operation at the same airflow, and the incremental energy cost relative to the field-tested 3-ACH operation (+4.6 kWh per day) is the cost of the additional airflow rather than of the filter.

3.5 Sensitivity Analysis

Table 7 and Figure 9 summarize the OAT results. In both cases the indoor-origin terms dominated: varying the indoor source strength by ±25% changed the mean indoor $PM_{2.5}$ by ±1.4 µg/m³ (±6.6%) in the Normal–MERV 13 case and by ±1.2 µg/m³ (±13%) in the Haze–HEPA case, and varying L(0) between 20 and 40 mg/m² changed it by ±1.3 and ±1.1 µg/m³, respectively. Deposition had a smaller effect (≤0.4 µg/m³), and envelope leakage and particle penetration changed the mean by less than 0.1 µg/m³ (<1%) because positive pressure kept the classroom exfiltrating, so that little unfiltered outdoor air entered. Compliance in the marginal Normal-MERV 13-5 ACH case varied from 71% to 92% across the sensitivity cases (82% at base), whereas the Haze-HEPA-6 ACH case remained at 100% in every case (highest mean 10.6 µg/m³), and CO_2 was unaffected (±1 ppm). The HEPA recommendation is therefore robust to the main input uncertainties, while conclusions for marginal configurations depend chiefly on how the indoor sources are characterized.

Table 7. One-at-a-time sensitivity of occupied-period $PM_{2.5}$ ($\Delta PM_{2.5}$ in µg/m³ relative to the base case)

Parameter	Low / Base / High	Normal-MERV 13-5 ACH			Haze-HEPA-6 ACH		
		$\Delta PM_{2.5}$ Low	$\Delta PM_{2.5}$ High	$PM_{2.5}$ ≤25 (%)	$\Delta PM_{2.5}$ Low	$\Delta PM_{2.5}$ High	$PM_{2.5}$ ≤25 (%)
Base case	-	-	-	82 (21.8 µg/m³)	-	-	100 (9.4 µg/m³)
Indoor $PM_{2.5}$ source	15,000 / 20,000 / 25,000 µg/h	-1.44	+1.44	88 / 71	-1.21	+1.21	100
Floor loading L(0)	20 / 30 / 40 mg/m²	-1.34	+1.34	92 / 74	-1.13	+1.13	100
Deposition rate	0.1 / 0.2 / 0.3 h^{-1}	+0.42	-0.40	79 / 85	+0.15	-0.14	100
Penetration factor P	0.6 / 0.8 / 1.0	-0.02	+0.02	82	-0.08	+0.08	100
Envelope leakage	×0.75 / ×1 / ×1.25	+0.01	-0.01	82	-0.06	+0.06	100

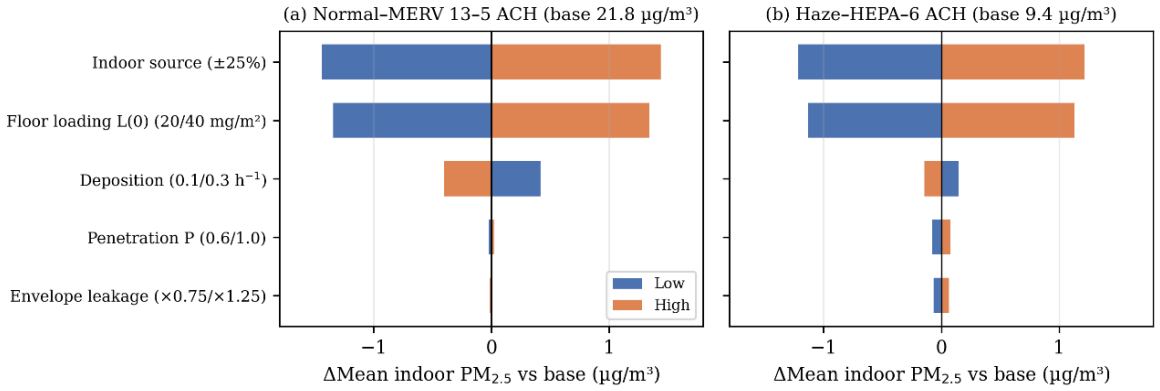

Figure 9. One-at-a-time sensitivity of occupied-period mean indoor $PM_{2.5}$ for (a) Normal-MERV 13-5 ACH and (b) Haze-HEPA-6 ACH; bars show the change from the base case at the Low and High level of each input

4. CONCLUSIONS

A CONTAM multizone model of a Bangkok classroom, calibrated against a measured positive-pressure ventilation dataset and independently validated against a second classroom, was used to evaluate 24 combinations of outdoor $PM_{2.5}$ condition, airflow rate, and filter grade under identical meteorological boundary conditions. Three findings stand out. First, CO_2 control was governed by airflow alone: occupied-time compliance rose from 32% at 3 ACH and 40% at 4 ACH to 96-97% at 5-6 ACH, so at least 5 ACH is required. Second, $PM_{2.5}$ control depended on filter grade and outdoor severity: HEPA kept indoor $PM_{2.5}$ within the guideline 90-100% of the time under both conditions (I/O

≈ 0.10-0.19 under haze), whereas MERV 13 was marginal under normal conditions (37-89%) and both MERV grades failed under haze. Third, because weather was held constant, total energy was dominated by outdoor-air cooling, was largely insensitive to filter grade, and depended only on airflow rate (6.5-13.6 kWh per day), identically for both conditions—so the energy cost of haze protection is the cost of the additional airflow rather than of the filtration. The recommended operation is therefore HEPA at 5 ACH under both normal and haze conditions, which met both guidelines 96% of occupied time at 11.1 kWh per day; the sensitivity analysis showed that HEPA protection was robust to the main input uncertainties, with indoor $PM_{2.5}$ most sensitive to the indoor source strength and floor loading. The main limitations are the use of a single representative classroom, a scope restricted to $PM_{2.5}$ and CO_2, reliance on assumed leakage and filter-efficiency values, single-day calibration and validation datasets measured under one operating condition, and CONTAM's well-mixed-zone assumption, which yields room-average rather than spatially resolved concentrations. Within these limits, the framework offers practical, transferable guidance for climate-resilient classroom ventilation in Bangkok and other Southeast Asian cities affected by seasonal haze.

Acknowledgement

The authors gratefully acknowledge the Department of Environmental and Sustainable Engineering and the Department of Mechanical Engineering, Faculty of Engineering, Chulalongkorn University, for their support of this research. The authors also gratefully acknowledge the financial support provided through Chulalongkorn University's Graduate Scholarship Program for ASEAN or Non-ASEAN Countries.

References

[1] Sadrizadeh, S., Yao, R., Yuan, F., Awbi, H., Bahnfleth, W., Bi, Y., ... Li, B. (2022). Indoor air quality and health in schools: A critical review for developing the roadmap for the future school environment. Journal of Building Engineering, 57, 104908.

[2] Ezeamii, V. C., Egbuchiem, A. N., Obianyo, C. M., Nwoke, P., & Okwuonu, L. (2025). Air quality monitoring in schools: Evaluating the effects of ventilation improvements on cognitive performance and childhood asthma. Cureus, 17(5), e83306.

[3] Stafford, T. M. (2015). Indoor air quality and academic performance. Journal of Environmental Economics and Management, 70, 34-50.

[4] Ongwandee, M., Khianthongkul, K., Panyametheekul, S., Yongprapat, K., Srinaka, K., & Morris, J. (2024). Bangkok school indoor air quality: Monitoring and intervention by positive pressure fresh air system. Environmental Science and Pollution Research, 31(17), 25454–25467.

[5] Agence France-Presse. (2025, January 24). Pollution-hit Bangkok closes hundreds of schools and offers free public transport. The Guardian.

[6] Bangkok Post. (2025, January 24). Bangkok air pollution forces 352 schools to close. Bangkok Post.

[7] Chiesa, G., & Vigliotti, M. (2024). Comparing mechanical ventilation control strategies for indoor air quality: Monitoring and simulation results of a school building in northern Italy. Energy and Buildings, 322, 114665.

[8] Na, H., Choi, H., Kim, H., Park, D., Lee, J., & Kim, T. (2023). Optimizing indoor air quality and noise levels in old school classrooms with air purifiers and HRV: A CONTAM simulation study. Journal of Building Engineering, 73, 106645.

[9] Won, Y., Chen, W., Wang, Z.-M., Wagner, J., & Kumagai, K. (2026). Analysis of impact of ventilation and air cleaning strategies on classroom $PM_{2.5}$ and CO_2 under normal and wildfire conditions – A CONTAM simulation study. Indoor Environments, 3(1), 100158.

[10] Shi, Y., Li, X., & Sadatiseyedmahalleh, S. (2020). Influence of building envelope type on the minimum mechanical ventilation rate to achieve a positive indoor air pressure. E3S Web of Conferences, 172, 05002.

[11] Dols, W. S., & Polidoro, B. (2020). CONTAM user guide and program documentation version 3.4 (NIST TN 1887). National Institute of Standards and Technology, Gaithersburg, MD.

[12] ASHRAE. (2021). ASHRAE handbook—Fundamentals. American Society of Heating, Refrigerating and Air-Conditioning Engineers, Atlanta, GA.

[13] Lawrie, L. K., & Crawley, D. B. (2026). Climate.OneBuilding.Org: Repository of free climate data for building performance simulation.

[14] Persily, A., & de Jonge, L. (2017). Carbon dioxide generation rates for building occupants. Indoor Air, 27(5), 868–879.

[15] Wu, Y., Li, Y., Gao, S., Liu, S., Yin, H., & Zhai, Y. (2023). Carbon dioxide generation rates for children and adolescents. Building and Environment, 237, 110310.

[16] ASHRAE. (2025). ANSI/ASHRAE Standard 52.2-2025: Method of testing general ventilation air-cleaning devices for removal efficiency by particle size. ASHRAE, Peachtree Corners, GA.
[17] ASHRAE. (2014). Guideline 14-2014: Measurement of energy, demand, and water savings. ASHRAE, Atlanta, GA.
[18] Silva, S., Monteiro, A., Russo, M. A., Valente, J., Alves, C., Nunes, T., ... Miranda, A. I. (2017). Modelling indoor air quality: Validation and sensitivity. Air Quality, Atmosphere & Health, 10(5), 643-652.
[19] Department of Health. (2022). Notification of indoor air quality guidelines for public buildings B.E. 2565 (2022). Ministry of Public Health, Thailand.
[20] World Health Organization. (2021). WHO global air quality guidelines: Particulate matter ($PM_{2.5}$ and PM_{10}), ozone, nitrogen dioxide, sulfur dioxide and carbon monoxide. WHO, Geneva.
[21] Chen, C., & Zhao, B. (2011). Review of relationship between indoor and outdoor particles: I/O ratio, infiltration factor and penetration factor. Atmospheric Environment, 45(2), 275-288.
[22] Alameddine, I., Gebrael, K., Hanna, F., & El-Fadel, M. (2022). Quantifying indoor $PM_{2.5}$ levels and its sources in schools: What role does location, chalk use, and socioeconomic equity play? Atmospheric Pollution Research, 13(3), 101375.
[23] Eom, Y. S., Park, B. R., Shin, H. W., & Kang, D. H. (2021). Evaluation of outdoor particle infiltration into classrooms considering air leakage and other building characteristics in Korean schools. Sustainability, 13(13), 7382.
[24] Taylor, J., Shrubsole, C., Davies, M., Biddulph, P., Das, P., Hamilton, I., Vardoulakis, S., Mavrogianni, A., Jones, B., & Oikonomou, E. (2014). The modifying effect of the building envelope on population exposure to $PM_{2.5}$ from outdoor sources. Indoor Air, 24(6), 639-651.
[25] Benabed, A., & Boulbair, A. (2022). PM10, PM2.5, PM1, and PM0.1 resuspension due to human walking. Air Quality, Atmosphere & Health, 15, 1547-1556.
[26] Liu, D.-L., & Nazaroff, W. W. (2003). Particle penetration through building cracks. Aerosol Science and Technology, 37(7), 565–573.
[27] Allen, R., Larson, T., Sheppard, L., Wallace, L., & Liu, L.-J. S. (2003). Use of real-time light scattering data to estimate the contribution of infiltrated and indoor-generated particles to indoor air. Environmental Science & Technology, 37(16), 3484-3492.
[28] Diapouli, E., Chaloulakou, A., & Koutrakis, P. (2013). Estimating the concentration of indoor particles of outdoor origin: A review. Journal of the Air & Waste Management Association, 63(10), 1113-1129.